Measurement of crack-face friction in collapsed weak snow layers

A. van Herwijnen[1] and J. Heierli[2]

Received 17 August 2009; revised 5 October 2009; accepted 28 October 2009; published 4 December 2009.

[1] In this letter we analyze the frictional contact forces during and immediately after the collapse of a weak snowpack layer, when the sliding plane consists of the freshly collapsed and crushed, but not yet eroded granular debris of the weak layer. The results from thirty-four field experiments show that frictional contact forces per unit area are on the order of 0.6 times the normal stress, equivalent to a friction angle close to 30 degrees. The measurements show that there is a transient, sharp drop in the coefficient of friction during the collapse of the weak layer and relatively constant values afterwards. One implication of our findings is that the minimum angle for avalanche release does not depend on shear strength, as commonly thought, but results from crack-face friction which comes into play only as the fracture through the weak layer is already propagating.
Citation: van Herwijnen, A., and J. Heierli (2009), Measurement of crack-face friction in collapsed weak snow layers, *Geophys. Res. Lett.*, *36*, L23502, doi:10.1029/2009GL040389.

1. Introduction

[2] An essential stage in the release of a dry snow slab avalanche is fracture propagation through a weak snowpack layer located below a slab-like layer of well-bonded snow [*Schweizer et al.*, 2003]. Experimental research has shown that the propagation of fracture involves the crushing of a weak snowpack layer [*Schweizer et al.*, 1995; *Johnson et al.*, 2004; *van Herwijnen and Jamieson*, 2005; *van Herwijnen et al.*, 2008]. Mathematically, the crushing process can be described as the propagation of a mixed-mode anticrack [*Heierli et al.*, 2008], in which the displacement field at the fracture front is equal in magnitude but opposite in sign to that of a classical tensile crack [*Fletcher and Pollard*, 1981]. As the fracture propagates, the slab progressively looses its support and comes into frictional contact with the bed surface through the weak layer debris. In the area of contact, the sliding motion of the slab is constrained by frictional forces which have, so far, received little experimental attention.

[3] Field observations show that dry snow slab avalanches rarely release on slopes inclined less than 30° [e.g., *Schweizer and Jamieson*, 2001]. However, numerous field observations show that fractures can propagate through weak snowpack layers on low-angle terrain, resulting in a sudden subsidence of the snowpack and produce a characteristic 'whumpf' sound. Slab avalanches may also be released on steep slopes after having been triggered by a person traveling on horizontal terrain [e.g., *Johnson and Jamieson*, 2001]. These observations demonstrate the existence of a minimum slope angle for slab avalanche release but none for fracture propagation. The reasons behind these observations are investigated in this letter by measuring friction during and after weak layer fracture propagation.

[4] Experimental studies have been performed by measuring the friction between samples of homogeneous snow [*Casassa et al.*, 1989, 1991] or by studying the effect of crack face friction on shear cracking in homogeneous snow samples [*Kirchner et al.*, 2002]. Thus far there are no studies on friction of fresh crack faces consisting of debris of fractured weak layers. In shear models of weak layer failure and slab avalanche release, frictional contact forces between crack faces are quite often neglected or assumed to be small [e.g., *Louchet et al.*, 2002; *Chiaia et al.*, 2008]. However, this assumption is neither based on experimental evidence nor is it unequivocal since for shear fractures the crack faces are always in contact due to gravity.

2. Methods

[5] For this study we used video sequences of snow samples sliding down-slope after failure of the weak layer to determine the amount of friction involved. The experiments were carried out in the mountains of British Columbia, Canada, during the winters of 2002–2003 and 2003–2004 and in the mountains in the region of Davos, Switzerland, during the winter of 2008–2009.

[6] Video sequences were recorded on fourteen different days in ten rutschblock tests (RB) [e.g., *Jamieson and Johnston*, 1993], twenty-one propagation saw tests (PST) [e.g., *Gauthier and Jamieson*, 2008b] and on three skier-tested slopes (ST) [*van Herwijnen and Jamieson*, 2005]. In all these tests, one side of the isolated snow sample was completely exposed by shoveling and black markers were placed in the vertical snow wall above the weak layer to analyze the motion of the slab (Figure 1). The experiments performed in Canada were recorded with a MotionMeter high-speed camera recording at 250 frames per second (fps) with a resolution of 344 x 264 pixels. The experiments preformed in Switzerland were recorded with a VDS Vosskhler HCC-1000 high-speed camera recording at 307 fps with a resolution of 1024 × 512 pixels or with a Canon Powershot G7 digital camera at 15 fps with a resolution of 1024 × 768 pixels.

[7] Particle tracking software [*Crocker and Grier*, 1996] was used to analyze the motion of the markers using a coordinate system as defined in Figure 1: the *x*-axis pointing in down-slope direction parallel to the snow surface, the

[1]WSL Institute for Snow and Avalanche Research SLF, Davos-Dorf, Switzerland.
[2]Institut für Zuverlässigkeit von Bauteilen und Systemen, Universität Karlsruhe, Karlsruhe, Germany.

0094-8276/09/2009GL040389

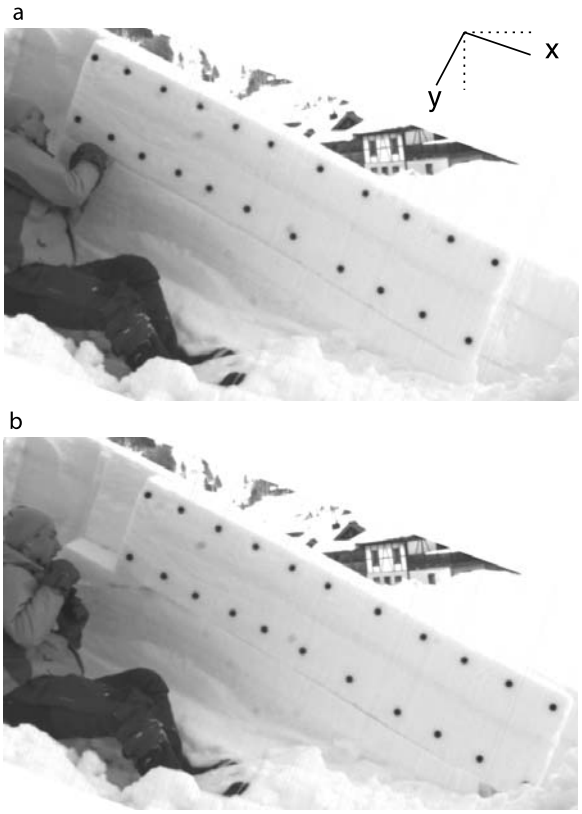

Figure 1. Shown here are the (a) first and (b) last image of video sequence propagation saw test C5. The coordinate system used in the particle image velocimetry analysis is also shown.

y-axis pointing towards the ground normal to the snow surface (Figure 1). The instant displacements $u_x(t)$ and $u_y(t)$ of each marker, were measured with reference to the initial positions x_0 and y_0 before fracture. The instant velocities $v_x(t)$ and $v_y(t)$ were obtained by numerical derivation of u_x and u_y using the first-order forward scheme $v_i(t) = [u_i(t + \Delta t) - u_i(t)]/\Delta t$ with Δt the time interval between two subsequent frames. The video sequences recorded in Canada had much more noise than those recorded in Switzerland. A seven point moving average filter was used to reduce fluctuations in the displacement data [*van Herwijnen and Jamieson*, 2005].

[8] In most experiments, after the initial subsidence of the slab during collapse of the weak layer, the down-slope sliding of the slab resulted in a secondary subsidence caused by the erosion of the weak layer debris or adjacent snow. The secondary subsidence rate $\dot{y}$ was calculated as the average slope normal velocity of the markers after fracture propagation. In some PST tests (indicated by 'b' in Table 1) fracture propagation through the weak layer arrested at a transverse fracture through the slab and only a small portion of the slab underwent longitudinal displacement. Furthermore, in some experiments (indicated by 'c' in Table 1) the secondary subsidence was not measurable since the slab decelerated and quickly came to a rest after a few cm of down-slope displacement.

[9] An average coefficient of friction was calculated from the acceleration of the slab after weak layer failure. According to experimental results obtained by *Casassa et al.* [1991] on the friction between blocks of snow, we assumed Coulomb-type friction. The average slope-parallel acceleration of the slab a in a given time interval I, was determined by fitting a to the equation for uniform acceleration $v_x(t) = v_0 + at$, $t \in I$, where v_0 is the initial slope parallel velocity. For $a \neq 0$, the average coefficient of friction μ is given by $\mu = \tan\theta - a/(g \cos\theta)$, where g is the acceleration of gravity and θ the slope angle. Alternatively, for some short video sequences recorded with the standard digital camera at 15 fps, the average slope-parallel acceleration of the slab was determined by fitting a to the slope parallel displacement for the entire video sequence after failure, i.e., $u_x(t) = \frac{1}{2} at^2$.

[10] For several high-speed camera sequences with high quality images, the increased temporal resolution allowed for a detailed observations of the instant coefficient of friction and the instant subsidence of the slab. The instant coefficient of friction, including during failure of the weak layer, was determined by reducing the time interval I to 10

Table 1. Overview of Experimental Parameters and Measured Coefficient of Friction and Erosion Rate[a]

Test	Type	fps	θ	WL	μ	$\dot{y}$ (cm s^{-1})
A1[b,c]	PST	15	28	SH	0.57	∼
A2[b,c]	PST	15	28	SH	0.59	∼
A3[b,c]	PST	15	31	SH	0.58	∼
A4[b]	PST	15	31	SH	0.57	1.3
A5[b]	PST	15	31	SH	0.52	2.4
A6[b]	PST	15	31	SH	0.54	1.6
A7[b]	PST	15	31	SH	0.55	0.5
A8[b]	PST	15	31	SH	0.53	3.4
A9[b]	PST	15	31	SH	0.56	1.0
A10[b,c]	PST	15	31	SH	0.58	∼
B1	PST	15	35	DH	0.58	2.4
B2	PST	15	35	DH	0.58	7.0
B3[b]	PST	15	35	DH	0.55	5.2
B4	PST	15	35	DH	0.58	5.9
C1[c]	PST	307	33	SH	0.68	∼
C2	PST	307	33	SH	0.56	2.4
C3[c]	PST	307	32	SH	0.64	∼
C4	PST	307	34	SH	0.57	2.6
C5	PST	307	33	SH	0.58	1.9
D[c]	PST	307	28	DH	0.58	∼
E1[c]	RB	250	30	SH	0.66	∼
E2[c]	RB	250	30	SH	0.64	∼
F[c]	PST	250	30	SH	0.60	∼
G1	RB	250	38	SH	0.57	1.8
G2	ST	250	38	SH	0.56	0.9
H	ST	250	34	DH	0.56	3.8
I1	RB	250	38	SH	0.57	1.6
I2	RB	250	38	SH	0.55	0.8
J1	ST	250	35	SH	0.57	1.0
J2	RB	250	38	SH	0.53	2.2
K	RB	250	33	SH	0.58	0.9
L1	RB	250	32	FC	0.61	1.2
L2[c]	RB	250	28	FC	0.68	∼
M	RB	250	30	SH	0.54	4.8

[a]Type: rutschblock (RB), propagations saw test (PST) or skier-tested slope (ST); fps: frame rate of the recording; θ: slope angle in degrees; WL: crystal type of the weak layer, i.e., buried surface hoar (SH), depth hoar (DH) or facetted crystals (FC); μ: average friction coefficient; $\dot{y}$: average erosion rate.

[b]Experiments in which a transverse fracture through the slab arrested fracture propagation.

[c]Experiments in which the slab quickly came to a rest after fracture propagation.

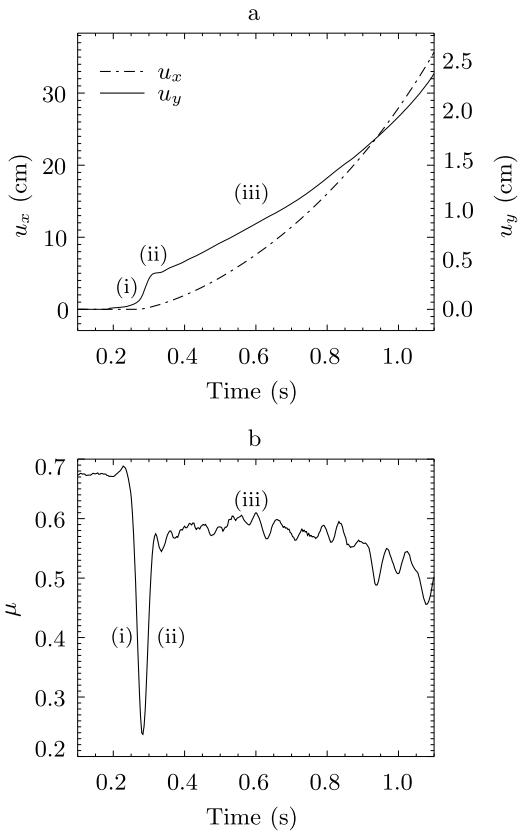

Figure 2. Example of measured displacement and coefficient of friction for experiment C5. (a) Slope parallel (dashed line) and slope normal (solid line) displacement averaged over all markers; note the different scales on the y-axis. (b) Corresponding coefficient of friction. Three stages during the experiment are highlighted: (i) collapse of the weak layer; (ii) first crack face contact; (iii) down-slope sliding of the slab.

video frames centered around t. The instant subsidence $\dot{y}(t)$ was determined using the same procedure.

3. Results

[11] The measured coefficients of friction for weak snowpack layers varied from 0.52 to 0.68 with a mean value of 0.57 (Table 1), corresponding to friction angles ranging from 27 to 34 degrees. After collapse, the rate of subsidence caused by erosion varied from 0.5 to 7.0 cms^{-1} with a mean value of 2.5 cms^{-1}. The calculated coefficients of friction and subsidence rates were independent of the test method (KW-test, p = 0.70 and p = 0.94, respectively), indicating that the measurements were not influenced by the experimental setup. The coefficient of friction was significantly larger in experiments where the slab came to a rest (n = 11; mean of 0.62) than in experiments where the slab slid down-slope (n = 23; mean of 0.56; T-test, $p = 10^{-6}$).

[12] The effect of normal load on the calculated coefficient of friction was determined in experiments A1 to A4. These tests were performed in close vicinity to each other. Weight was removed by cutting a layer of snow from the surface or was added on top of the slab in the form of blocks of snow. The data show that the calculated coefficients of friction did not depend on the loading, as expected for Coulomb-type friction (Table 1, A1–A4).

[13] The instant coefficient of friction for experiment C5 shows that the collapse of the weak layer caused a sudden drop in the coefficient of friction, indicated by (i) in Figure 2. After completed collapse, the coefficient of friction rapidly increased, indicated by (ii) in Figure 2. After the fracture had propagated through the entire sample, the slab started to slide resulting in erosion of the weak layer debris. The acceleration of the slab indicates a constant or slowly deceasing coefficient of friction, indicated by (iii) in Figure 2. In all experiments where the slab slid away after fracture propagation the coefficient of friction exhibited the same characteristic evolution as in experiment C5 (Figure 3a).

[14] The instant subsidence $\dot{y}$ attained a maximum during collapse of the weak layer (Figure 3b). Thereafter, $\dot{y}$ was relatively constant or increased with increasing slope parallel velocity of the slab. In Figure 3b, $\dot{y}$ was largest for experiment H and the largest erosion rates shown in Table 1 were for experiments B2, B3 and B4. These experiments were performed on thick weak layers of basal depth hoar. It comes as no surprise that the erosion of such weak layers is largest since layers of depth hoar are generally very porous and have low cohesion.

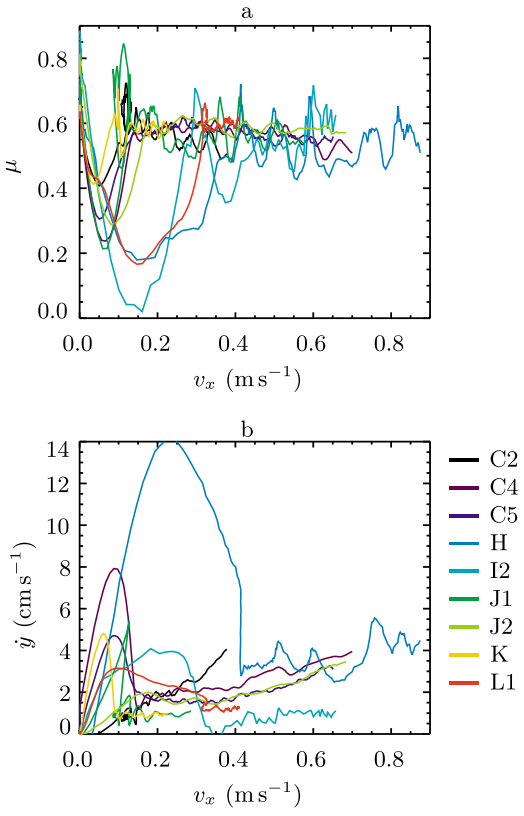

Figure 3. Variation in the coefficient of friction and the slope normal subsidence with slope parallel velocity of the slab for experiments in which the slab moved down-slope. (a) Instant coefficient of friction. (b) Corresponding instant slope normal subsidence. The colors of the curves represent the different experiments, as indicated in the legend.

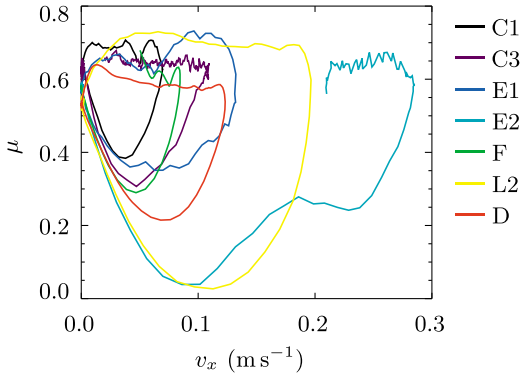

Figure 4. Variation in the instant coefficient of friction with slope parallel velocity of the slab for experiments in which the slab quickly came to a rest. The colors of the curves represent the different experiments, as indicated in the legend.

[15] For experiments where the slab came to a rest after fracture propagation the evolution of the coefficient of friction is shown in Figure 4. Again, the collapse of the weak layer coincided with a rapid decrease followed by a rapid increase of μ. However, after the weak layer had failed, the slab decelerated and came to a stop. The instant coefficient of friction during this process was generally constant and, as mentioned before, significantly larger than in the other experiments.

4. Discussion and Conclusion

[16] Field measurements were carried out in order to determine the amount of friction of a freshly debonded slab on a bed of weak layer debris, during and immediately after the collapse of the weak layer. The results indicate that crack-face friction in collapsed weak layers is far from negligible. The measured coefficients of friction after fracture propagation had a mean value of 0.57, comparable in magnitude to previously published values for snow-to-snow contacts [*Casassa et al.*, 1989, 1991]. The friction data presented in this letter showed no dependance on grain type of the weak layer. However, it is still possible that friction depends on snow stratigraphy, in particular on the grain type and hardness of the weak layer as well as the layer above and below it.

[17] During fracture propagation the weak layer collapses and the slab looses its support and subsides. The measurements show an abrupt drop of the friction coefficient during the collapse phase, followed by a sharp increase after completed collapse and, subsequently, either a constant or a slightly decreasing coefficient of friction was observed (Figures 2, 3, and 4).

[18] The measurements presented in this letter were obtained under the assumption of Coulomb-type friction. This assumption is corroborated by the independence of the acceleration under different loads (Table 1, A1–A4) and the relative constant values of the friction coefficients under increasing sliding velocity. The decrease in the coefficient of friction with increasing velocity is likely caused by the erosion of the weak layer debris and adjacent snow which undoubtedly smoothes the crack faces and therefore reduces frictional contact forces.

[19] Crack-face friction is an important parameter for theoretical models of slab avalanche release. For many years the theory of slab avalanche release was based on the formation and propagation of a shear crack within the weak layer [e.g., *Louchet et al.*, 2002; *McClung*, 1979]. According to such models the propagation of a shear crack is not possible on slopes inclined below the friction angle [*Heierli et al.*, 2008], which according to the measurements presented here is close to 30°. However, field observations of whumpfs and remotely triggered avalanches as well as previously published experimental results [*Gauthier and Jamieson*, 2008a; *van Herwijnen and Jamieson*, 2005; *van Herwijnen et al.*, 2008] and those in Table 1 show that fractures often propagate on slope with an inclination below the friction angle and even on horizontal terrain. This is in sharp contrast to the predictions of the shear model.

[20] This inconsistency is resolved by the anticrack model for slab avalanche release which incorporates the collapse of the weak layer [*Heierli et al.*, 2008]. In this model, the fracture process can occur with or without shear loading and for arbitrary amounts of crack-face friction, providing an explanation for fracture propagation in slopes inclined by less than the friction angle. Combined with Coulomb-type friction, the anticrack model indicates a sharp threshold for the whumpf-avalanche transition. Immediately below the friction angle, fracture propagation results in a whumpf. Immediately above the friction angle a slab avalanche is released. There is no gradual increase of hazard with slope angle as in the shear model, but an immediate transition from whumpfing to avalanching.

[21] In reality, it is likely that the resistance to slab motion is not entirely controlled by crack-face friction. The snow in place around the debonded slab, in particular the stauchwall (i.e., the down-slope boundary of the slab) and roughness of the bed surface, stabilizes the slab against down-slope motion. Thus, the net pull on the slab must not only overcome crack-face friction but also some additional resistance from the periphery of the slab and the roughness of the bed. Hence the critical slope angle for the whumpf-avalanche transition is expected to be somewhat larger than the friction angle.

[22] An important implication of our findings is that the minimum angle for avalanche release does not depend on shear strength, as is often thought, but results from crack-face friction which comes into play only as the fracture through the weak layer is already propagating. Therefore, valuable snowpack stability information with regards to fracture initiation and fracture propagation can be obtained on gentle slopes and even on horizontal terrain (without regard of the subsequent friction problem). Practitioners have known and applied this idea for a long time. A practical implication of our findings is that skiers and snowboarders should be aware of abrupt changes in risk with small variations in slope angle in the neighborhood of the friction angle.

[23] **Acknowledgments.** We thank Bruce Jamieson, Applied Snow and Avalanche Research (ASARC), University of Calgary, for making the Canadian data available. We thank Michael Zaiser for useful discussions. The financial support of the European Commission under contract NEST-2005-PATH-COM-043386 is gratefully acknowledged.

References

Casassa, G., H. Narita, and N. Maeno (1989), Measurement of friction coefficients of snow blocks, *Ann. Glaciol.*, *13*, 40–44.

Casassa, G., H. Narita, and N. Maeno (1991), Shear cell experiments of snow and ice friction, *J. Appl. Phys.*, *69*, 3745–3753.

Chiaia, B. M., P. Cornetti, and B. Frigo (2008), Triggering of dry snow slab avalanches: Stress versus fracture mechanical approach, *Cold Reg. Sci. Technol.*, *53*, 170–178.

Crocker, J., and D. Grier (1996), Methods of digital video microscopy for colloidal studies, *J. Colloid Interface Sci.*, *179*, 298–310.

Fletcher, R. C., and D. D. Pollard (1981), Anticrack model for pressure solution surfaces, *Geology*, *9*, 419–424.

Gauthier, D., and B. Jamieson (2008a), Evaluation of a prototype field test for fracture and failure propagation propensity in weak snowpack layers, *Cold Reg. Sci. Technol.*, *51*, 87–97.

Gauthier, D., and B. Jamieson (2008b), Fracture propagation propensity in relation to snow slab avalanche release: Validating the Propagation Saw Test, *Geophys. Res. Lett.*, *35*, L13501, doi:10.1029/2008GL034245.

Heierli, J., P. Gumbsch, and M. Zaiser (2008), Anticrack nucleation as triggering mechanism for slab avalanches, *Science*, *321*, 240–243.

Jamieson, J., and C. Johnston (1993), Rutschblock precision, technique variations and limitations, *J. Glaciol.*, *39*, 666–674.

Johnson, B., and B. Jamieson (2001), Field data and theory for human-triggered "whumpfs" and remote avalanches, paper presented at the 2000 International Snow Science Workshop, Am. Avalanche Assoc., Big Sky, Mont.

Johnson, B. C., J. B. Jamieson, and R. R. Stewart (2004), Seismic measurements of fracture speed in a weak snowpack layer, *Cold Reg. Sci. Technol.*, *40*, 41–45, doi:10.1016/j.coldregions.2004.05.003.

Kirchner, H. O., G. Michot, and J. Schweizer (2002), Fracture toughness of snow in shear under friction, *Phys. Rev. E*, *66*, 027103, doi:10.1103/PhysRevE.66.027103.

Louchet, F., J. Faillettaz, D. Daudon, N. Bédouin, E. Collet, J. Lhuissier, and A.-M. Portal (2002), Possible deviations from Griffith's criterion in shallow slabs, and consequences on slab avalanche release, *Nat. Hazards Earth Syst. Sci.*, *2*, 1–5.

McClung, D. M. (1979), Shear fracture precipitated by strain softening as a mechanism of dry avalanche release, *J. Geophys. Res.*, *84*, 3519–3526.

Schweizer, J., and J. Jamieson (2001), Snow cover properties for skier triggering of avalanches, *Cold Reg. Sci. Technol.*, *33*, 207–221.

Schweizer, J., M. Schneebeli, C. Fierz, and P. M. B. Föhn (1995), Snow mechanics and avalanche formation: Field experiments on the dynamic-response of the snow cover, *Surv. Geophys*, *16*(5–6), 621–633.

Schweizer, J., J. Bruce Jamieson, and M. Schneebeli (2003), Snow avalanche formation, *Rev. Geophys.*, *41*(4), 1016, doi:10.1029/2002RG000123.

van Herwijnen, A., and B. Jamieson (2005), High-speed photography of fractures in weak snowpack layers, *Cold Reg. Sci. Technol.*, *43*, 71–82.

van Herwijnen, A., J. Heierli, and J. Schweizer (2008), Field study on fracture propagation in weak snowpack layers, paper presented at the 2008 International Snow Science Workshop, Am. Avalanche Assoc., Whistler, B. C., Canada.

J. Heierli, Institut für Zuverlässigkeit von Bauteilen und Systemen, Universität Karlsruhe, Kaiserstr. 12, D-76131 Karlsruhe, Germany.

A. van Herwijnen, WSL Institute for Snow and Avalanche Research SLF, Flüelastr. 11, CR-7260 Davos-Dorf, Switzerland. (vanherwijnen@slf.ch)